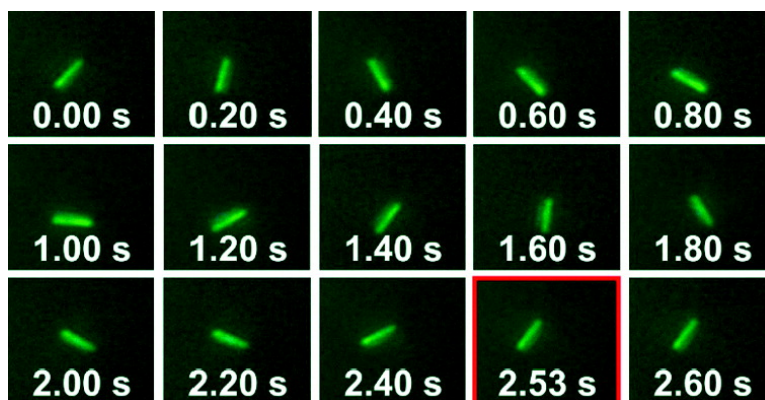


## Rational Design and Synthesis of Catalytically Driven Nanorotors

Lidong Qin, Matthew J. Banholzer, Xiaoyang Xu, Ling Huang, and Chad A. Mirkin

*J. Am. Chem. Soc.*, **2007**, 129 (48), 14870-14871 • DOI: 10.1021/ja0772391

Downloaded from <http://pubs.acs.org> on February 9, 2009



### More About This Article

Additional resources and features associated with this article are available within the HTML version:

- Supporting Information
- Links to the 12 articles that cite this article, as of the time of this article download
- Access to high resolution figures
- Links to articles and content related to this article
- Copyright permission to reproduce figures and/or text from this article

[View the Full Text HTML](#)

## Rational Design and Synthesis of Catalytically Driven Nanorotors

Lidong Qin, Matthew J. Banholzer, Xiaoyang Xu, Ling Huang, and Chad A. Mirkin\*

Department of Chemistry and International Institute for Nanotechnology, Northwestern University,  
2145 Sheridan Road, Evanston, Illinois 60208

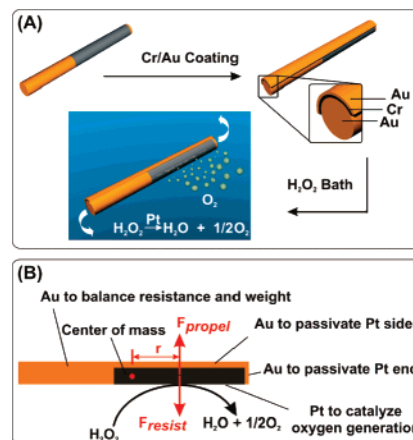
Received October 2, 2007; E-mail: chadnano@northwestern.edu

Chemically and catalytically powered nano-objects are a fascinating area of research. They have the potential to facilitate the development of nanomechanical devices that could find utility in microfluidics and drug delivery.<sup>1–11</sup> Over the past 3 years, several groups have studied how the catalytic decomposition of  $\text{H}_2\text{O}_2$  by multicomponent segmented nanorod structures (Pt–Au, Ni–Au) can drive nanomechanical systems.<sup>10–20</sup> Most of the systems studied thus far, such as in the work of Mano et al., Wang et al., Paxton et al., and Kline et al. have involved chemically powered linear motion,<sup>10,11,13,15,18</sup> although a couple of examples involve the spinning of structures tied to a surface at one end of a two-component, two-segment nanorod.<sup>16</sup> In another example, Catchmark et al. demonstrated rotational movement in a conventionally microfabricated microgear based on the same catalytic reactions, and Chang et al. demonstrated macro-object rotation via linked diodes.<sup>6,21</sup> Last, bent structures have been prepared by He et al. by “dynamic shadowing growth” that allow one to realize “boomerang-like” structures composed of Pt and Si. These impressive catalytically powered structures are capable of spinning, but the fabrication approach used to generate them is complex, low yielding in terms of functional structures, and does not provide fine control over the architectural parameters (compositional blocks, length, diameter) important to the controlled movement of such structures.<sup>22</sup>

Controlling the asymmetric forces involving these  $\text{H}_2\text{O}_2$  driven nanomotors is a major challenge. This control, which is essential for achieving a stable torque on these nano-objects, requires a precise method for adjusting the nanorod segment dimensions, compositions, and locations. On-wire lithography (OWL) has emerged as a method for tailoring the architecture of nanorod materials on the sub-5 nm to many micrometer length scale.<sup>23–25</sup> This approach, which is based upon template-directed synthesis,<sup>26–29</sup> not only allows one to control the composition of different segments along the long axis of the rod, but also allows one to coat one face of multicomponent rod structures with a desired material. We hypothesized that this capability would allow us to synthesize a set of structures with the proper compositional blocks and asymmetry to realize a new class of catalytically powered nanorotors (NR). As proof-of-concept, we synthesized Au–Pt–Au three-segment nanorods (diameter = 360 nm; first Au section length = 1.67  $\mu\text{m}$ , Pt section length = 3.33  $\mu\text{m}$ , second Au passivating section length = 20 nm) coated on one face with a Au/Cr bilayer (10 nm Cr/40 nm Au) via OWL (Scheme S1, see Supporting Information). These nanostructures leave only one side of the Pt segment exposed (Scheme 1A).

After synthesizing these structures, we studied their movement driven by the catalytic decomposition of  $\text{H}_2\text{O}_2$ . In a typical experiment, 10  $\mu\text{L}$  of an aqueous suspension of NRs (containing  $1 \times 10^5$  rotors) was mixed with 1 mL of 3%  $\text{H}_2\text{O}_2$ . A droplet of the mixture was promptly placed on a glass bottom dish and characterized by dark-field optical microscopy. Of the 500 NRs studied, 95% were actively rotating while the remaining 5% exhibited either

**Scheme 1.** (A) Schematic Diagram of the Synthesis of Au/Pt NR and Its Motion in a  $\text{H}_2\text{O}_2$  Bath. (B) Structure and Force Analysis of the Designed NR



random or linear motion, possibly due to structural defects generated during synthesis. This rotation of the NRs was recorded to determine the direction and speed of rotation (video S1, see Supporting Information).

In a representative sample of the  $\text{Au}_{1.67}\text{Pt}_{3.33}\text{Au}_{0.02}$  NRs, one can distinguish the Au and Pt sections based upon color and contrast (Figure 1). The yellow ends are the gold segments and the gray section is Pt. Time lapse dark field microscopy experiments show that a full turn of a NR is completed in 2.53 s corresponding to a rotation speed of 23.7 rpm, Figure 1. Note that the NRs can rotate in both a clockwise and counterclockwise direction, and the speed increases with increasing  $\text{H}_2\text{O}_2$  concentration up to 3%  $\text{H}_2\text{O}_2$ . At or above this concentration the reaction is limited by Pt surface area rather than peroxide concentration.

There have been two general classes of mechanisms proposed for nanorod locomotion. They can be differentiated by the direction in which the nanorod moves. In the first class, catalytic  $\text{H}_2\text{O}_2$  decomposition at a two component Au–Pt or Au–Si rod is proposed to explain cases in which the nanorod is pushed in the direction defined by the gold (or Si) end being the leading edge (the so-called “recoil mechanism”).<sup>16,22</sup> In the second class, the localized product concentration from  $\text{H}_2\text{O}_2$  decomposition creates either an electrofluidic gradient or an interfacial tension that results in the rod being pulled in the opposite direction toward the Au end.<sup>3,11,13,18,21</sup> Since the evaporated gold backings in our NRs are the leading edges during rotation, this second class of mechanisms does not fit our system (Video S2, Figure S3, see Supporting Information). To determine if the electrofluidic mechanism described above was in play in this system, we added  $\text{NaNO}_3$  to the solution (final concentration = 0.33 mM). The  $\text{NaNO}_3$  has been proposed to screen the NR’s  $\zeta$ -potential, which should minimize contributions defined via the electrofluidic mechanism.<sup>30</sup> The NR

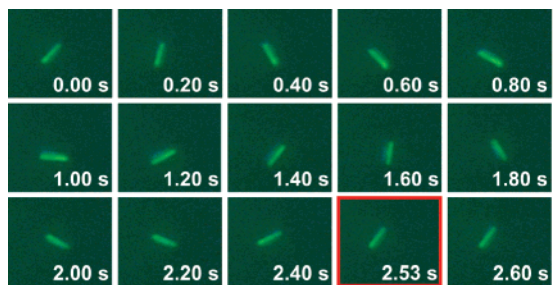


**Figure 1.** Snapshots of an Au–Pt–Au NR in 3% H<sub>2</sub>O<sub>2</sub>. The width of each frame is 20 μm. The rod moves in a counterclockwise manner.

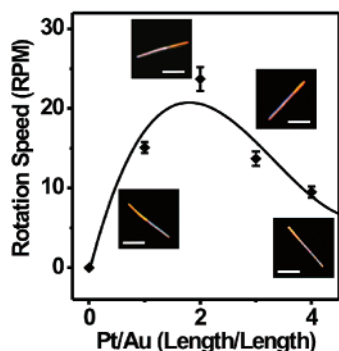


**Figure 2.** Recorded rotation speed vs length ratio of Pt/Au of a 5-μm NR in 3% H<sub>2</sub>O<sub>2</sub> bath. Inset: Dark field optical images of Au–Pt–Au nanorods with Pt/Au ratio of 1:1, 2:1, 3:1, and 4:1 from left to right. Scale bars are 2 μm.

rotation under these conditions was unaffected, implying the electrofluidic mechanism is not a significant contributor to rotation.

In this novel NR system, gas evolution generates a force that propels the structure, resulting in a net rotation. The movement of the whole structure is resisted by the fluid nearly uniformly across the NR long axis and can be described by a vector ( $F_{\text{resist}}$ ) directly opposing  $F_{\text{propel}}$  (Scheme 1B). During the initial stages of rotation,  $F_{\text{propel}} > F_{\text{resist}}$  (Scheme 1B). Since  $F_{\text{resist}}$  is dominated by drag forces, it is proportional to speed. At a critical speed,  $F_{\text{resist}} = F_{\text{propel}}$ , no net force is applied to the spinning rotor, and consequently angular velocity is constant.

The ability to use OWL to rationally design and precisely control the length and diameter of the rod and introduce the Au backing to break the symmetry of the structure makes it possible to systematically evaluate the architectural parameters that lead to the NR behavior described above. In particular, by varying the ratio of Pt to Au segment lengths, we are able to optimize rotation speed. Further, by positioning the Pt at different points along the nanowire we are able to fine-tune the amount of torque applied on the system. To illustrate these capabilities, 5 μm long NRs with Pt/Au length ratios of 1:1, 2:1, 3:1, and 4:1 were designed and synthesized. The corresponding rotation speeds were  $15.1 \pm 0.7$ ,  $23.7 \pm 1.5$ ,  $13.7 \pm 0.9$ , and  $9.5 \pm 0.7$  rpm, respectively, which were investigated by counting rotations by optical microscopy (Figure 2). A quasi-parabolic relationship between the speed and the segment length ratio was obtained, which clearly demonstrates that Pt/Au ratio plays an important role in the rotation speed. This can be understood by noticing the torque will vary with the amount and location of Pt present on the rod. When the applied torque is considered in combination with factors possibly affecting the nanorod (different surface/interface properties between Au and Pt, convection/fluid dynamics such as eddies effecting drag, etc., could all lead to nonideal behavior.) it appears that a 2:1 ratio of Pt/Au is nearly

optimal, even if this is not what is predicted by simple torque calculations alone.

In conclusion, we have designed and synthesized NRs based upon OWL. Due to the asymmetric structure of the NRs, they are able to rotate in a H<sub>2</sub>O<sub>2</sub> bath. By observing the leading edge of rotation and comparing this result to the NR design, we have concluded the driving force of the motion in this catalytically driven nanomotor system is the result of dynamic decomposition of H<sub>2</sub>O<sub>2</sub> to generate O<sub>2</sub>. We also discovered that the rotation speed in the NR system has a quasi-parabolic relationship with the Pt/Au ratio. The maximum rotation speed takes place very close to the Pt/Au ratio of 2.0. This work is a significant step toward systematic design of NRs and the described method opens a new avenue for generating nanomotors with more complex movement patterns.

**Acknowledgment.** This work was supported by the AFOSR, DARPA, and NSF. C.A.M. is grateful for a NIH Director's Pioneer Award.

**Supporting Information Available:** Experimental details and optical microscopy video images. This material is available free of charge via the Internet at <http://pubs.acs.org>.

## References

- (1) Fletcher, S. P.; Dumur, F.; Pollard, M. M.; Feringa, B. L. *Science* **2005**, *310*, 80–82.
- (2) Weibel, D. B.; Garstecki, P.; Ryan, D.; DiLuzio, W. R.; Mayer, M.; Seto, J. E.; Whitesides, G. M. *Proc. Natl. Acad. Sci. U.S.A.* **2005**, *102*, 11963–11967.
- (3) Ruckner, G.; Kapral, R. *Phys. Rev. Lett.* **2007**, *98*, 150631–150634.
- (4) Eelkema, R.; Pollard, M. M.; Vicario, J.; Katsonis, N.; Ramon, B. S.; Bastiaansen, C. M.; Broer, D. J.; Feringa, B. L. *Nature* **2006**, *440*, 163.
- (5) Fennimore, A. M.; Yuzvinsky, T. D.; Han, W.-Q.; Fuhrer, M. S.; Cumings, J.; Zettl, A. *Nature* **2003**, *424*, 408–410.
- (6) Chang, S. T.; Paunov, V. N.; Petsev, D. N.; Velev, O. D. *Nat. Mater.* **2007**, *6*, 235–240.
- (7) Regan, B. C.; Aloni, S.; Jensen; Ritchie, R. O.; Zettl, A. *Nano Lett.* **2005**, *5*, 1730–1733.
- (8) Li, J. J.; Tan, W. *Nano Lett.* **2002**, *2*, 315–318.
- (9) Chen, Y.; Wang, M.; Mao, C. *Angew. Chem., Int. Ed.* **2004**, *43*, 3554–3557.
- (10) Mano, N.; Heller, A. *J. Am. Chem. Soc.* **2005**, *127*, 11574–11575.
- (11) Wang, Y.; Hernandez, R. M., Jr.; D. J. B.; Bingham, J. M.; Kline, T. R.; Sen, A.; Mallouk, T. E. *Langmuir* **2006**, *22*, 10451–10456.
- (12) Ismagilov, R. F.; Schwartz, A.; Bowden, N.; Whitesides, G. M. *Angew. Chem., Int. Ed.* **2002**, *41*, 652–654.
- (13) Paxton, W. F.; Kistler, K. C.; Olmeda, C. C.; Sen, A.; Angelo, S. K. S.; Cao, Y.; Mallouk, T. E.; Lammert, P. E.; Crespi, V. H. *J. Am. Chem. Soc.* **2004**, *126*, 13424–13431.
- (14) Ozin, G. A.; Manners, I.; Fournier-Bidoz, S.; Arsenault, A. *Adv. Mater.* **2005**, *17*, 3011–3018.
- (15) Kline, T. R.; Paxton, W. F.; Mallouk, T. E.; Sen, A. *Angew. Chem., Int. Ed.* **2005**, *44*, 744–746.
- (16) Fournier-Bidoz, S. B.; Arsenault, A. C.; Manners, I.; Ozin, G. A. *Chem. Commun.* **2005**, 441–443.
- (17) Vicario, J.; Eelkema, R.; Browne, W. R.; Meetsma, A.; La Crois, R. M.; Feringa, B. L. *Chem. Commun.* **2005**, 3936–3938.
- (18) Paxton, W. F.; Sen, A.; Mallouk, T. E. *Chem. Eur. J.* **2005**, *11*, 6462–6470.
- (19) Paxton, W. F.; Sundararajan, S.; Mallouk, T. E.; Sen, A. *Angew. Chem., Int. Ed.* **2006**, *45*, 5420–5429.
- (20) Kung, H. H.; Kung, M. C. *Appl. Catal. A* **2006**, *309*, 159–161.
- (21) Catchmark, J. M.; Subramanian, S.; Sen, A. *Small* **2005**, *1*, 202–206.
- (22) He, Y.; Wu, J.; Zhao, Y. *Nano Lett.* **2007**, *7*, 1369–1375.
- (23) Qin, L.; Park, S.; Huang, L.; Mirkin, C. A. *Science* **2005**, *309*, 113–115.
- (24) Qin, L.; Jang, J.-W.; Huang, L.; Mirkin, C. A. *Small* **2007**, *3*, 86–90.
- (25) Qin, L.; Zou, S.; Xue, C.; Atkinson, A.; Schatz, G. C.; Mirkin, C. A. *Proc. Natl. Acad. Sci. U.S.A.* **2006**, *103*, 13300–13303.
- (26) Martin, C. R. *Science* **1994**, *266*, 1961–1966.
- (27) Nicewarner-Peña, S. R.; Freeman, G.; Reiss, B. D.; He, L.; Peña, D. J.; Walton, I. D.; Cromer, R.; Keating, C. D.; Natan, M. J. *Science* **2001**, *294*, 137–141.
- (28) Hurst, S. J.; Payne, E. K.; Qin, L.; Mirkin, C. A. *Angew. Chem., Int. Ed.* **2006**, *45*, 2672–2692.
- (29) Park, S.; Lim, J.-H.; Chung, S.-W.; Mirkin, C. A. *Science* **2004**, *303*, 348–351.
- (30) Mallouk, T. E. Pennsylvania State University. Private communication, Sep 27, 2007.

JA0772391